Transatlantic Journal of Multidisciplinary Research
(p-ISSN: 2672-5371) (e-ISSN:2735-9808)
Journal Homepage: https://tjmr.org/
Vol. 8(1) 2026

TJMR
Transatlantic Journal of
Multidisciplinary Research

| RESEARCH ARTICLE

Comparative Analysis Of Raw Crab Shell And Synthesized Chitin As Reinforcements For Unsaturated Polyester Resin

Anyanwu P.I, Iheaturu N.C, Akanbi M.N, Aharanwa B.C. , Obeta M.C
Department of Polymer Engineering, Federal University of Technology, Owerri, Imo State

Corresponding Author: E-mail: placid.anyanwu@futo.edu.ng

| ABSTRACT

This study investigates the transition of industrial marine waste from a low-grade filler to a high-performance reinforcement through chemical refinement. Unsaturated polyester (UPE) resin composites were fabricated using raw crab shell (CRS) and synthesized chitin (CTN) at a 40:60 reinforcement-to-matrix weight ratio. Chitin was extracted via sequential demineralization and deproteinization, achieving a reduction in calcium content from 23.32 wt% to 16.38 wt% as verified by Energy Dispersive X-ray (EDX) spectroscopy. Fourier Transform Infrared (FTIR) spectroscopy confirmed the successful removal of carbonate bands and the purification of the chitin polymer backbone. Mechanical characterization revealed that while raw crab shell hindered performance due to poor interfacial bonding, the chitin-reinforced composites showed significant improvements in structural integrity. Furthermore, thermal analysis (TGA/DTA) identified raw crab shell as a thermal pro-degradant, whereas chitin provided a more stable degradation profile. Scanning Electron Microscopy (SEM) corroborated these findings, showing a transition from a fragmented, rocky interface in CRS composites to a better-integrated morphology in CTN composites. The results demonstrate that the chemical extraction of chitin is a critical step in adding value to crustacean waste for high-value engineering applications.

| KEYWORDS

Crab shell, Chitin, deproteination, demineralization

Introduction

The global pursuit of sustainable materials has shifted focus toward bio-fillers derived from agro and biological waste (Mohanty et al., 2018; Faruk et al., 2012). Among these, crustacean shells primarily from the crab processing industry represent a significant environmental challenge and an underutilized resource. Crab shells are often discarded as environmental pollutants, contributing to solid waste accumulation and unpleasant odors (Yan & Chen, 2015). However, these exoskeletons are rich in chitin, the second most abundant natural polysaccharide after cellulose (Rinaudo, 2006), which possesses high specific strength, biodegradability, and thermal stability (Pillai et al., 2009). The marine industry generates millions of tons of crustacean waste annually (Kucukgulmez et al., 2011). In Nigeria, particularly the coastal community in Rivers State, crab shells are a major environmental pollutant (Akarue & Akarue, 2020). However, this exoskeleton is a biological composite of chitin fibers embedded in a matrix of calcium carbonate and proteins (Muzzarelli, 1977; Rinaudo, 2006)

Unsaturated polyester (UPE) resin is a dominant thermosetting matrix in the automotive and construction industry due to its cost-effectiveness and ease of processing (Ku et al., 2011). Despite these advantages, neat UPE is inherently brittle and prone to volumetric shrinkage during curing (Ramesh et al., 2017). While synthetic reinforcements like glass or carbon fibers are commonly used to mitigate these flaws, the high cost and negative environmental impact have attracted renewed interest in bio-based alternatives (Faruk et al., 2012; Mohanty et al., 2018).

Traditional composites rely on synthetic fibers (glass, aramid) which cause respiratory issues and skin irritation during manufacturing (Sanjay et al., 2018). Natural fillers like crab shell derivatives offer a waste-to-wealth solution. Chitin ($C_8H_{13}NO_5$) is a high-molecular-weight linear polymer of N-acetyl-D-glucosamine (Rinaudo, 2006; Pillai et al., 2009). Literature suggests that while inorganic fillers (like $CaCO_3$) found in raw shells can increase stiffness, they often degrade the polymer's thermal stability if not properly integrated (Demir et al., 2006). This study focuses on the chemical extraction method (demineralization and deproteinization) as the primary pathway to enhance filler-matrix compatibility (Abdou et al., 2008; Islam et al., 2011).

Existing literature has explored the use of various calcium-rich bio-wastes (such as eggshells and snail shells) as fillers (Onuegbu et al., 2011; Oladele et al., 2019), but few studies provide a direct comparative analysis of the raw crab exoskeleton versus its chemically refined derivative, chitin, within a UPE matrix. The primary challenge in using raw shells lies in their complex composition—consisting of calcium carbonate, proteins, and lipids which often leads to poor interfacial adhesion with the polymer matrix (Ku et al., 2011; Nwosu et al., 2022 This paper aims to bridge this gap by examining how the chemical removal of minerals and proteins influences the thermo-mechanical synergy between the filler and the UPE resin. By comparing the mechanical properties (tensile and hardness), thermal stability (TGA), and microstructural evolution (SEM/EDX) of crab shell and chitin composites (Demir et al., 2006; Abdou et al., 2008), this research establishes the necessity of chemical refinement in transforming hazardous waste into a viable, eco-friendly reinforcement for modern composite manufacturing (Mohanty et al., 2018; Yan & Chen, 2015).

2.0 Experimental

Materials: Raw crab shells from Rivers State, UPE resin, Cobalt Naphthanate (accelerator), and MEKP (catalyst).

Chitin Extraction:

Demineralization:

Demineralization was carried out at room temperature according to the process described by Puvvada Y.S. et al, (2012), and Isa M. T. et al, (2012).

The process involved washing the crab shells with prepared 1% HCl several times until evolution of gas ceased. Crab shells were washed 10 – 15 times with approximately 20 liters of prepared 1% HCl solution. The crabs were further washed with distilled water repeatedly until a neutral pH was obtained and further dried at 60ºC.

Deproteinization:

Deproteinization was carried out on the dried crab shells by bathing in 2% NaOH severally until absence of bright red colour was observed. It was further soaked in 2% NaOH for 24hours and further rinsed with distilled water and dried at 60oC to constant weight.

Composite Fabrication: Samples were produced using the hand lay-up technique. The ratio for this mix is fixed at 40% Filler to 60% UPE.

Characterization: Mechanical testing (Instron UTM), Hardness (Vickers MV1-PC), FTIR (to track chemical changes), and SEM-EDX (to analyses the fracture surface and elemental shifts)

3.0 Results And Discussion (Crab Shell (Crs) Vs. Chitin (Ctn)

3.1 Chemical and Elemental Transition (EDX/FTIR)

The extraction process was validated by the significant shift in elemental composition shown in the EDX results for the composites.

S/N	**Element**	**Control UPE**	**CRS 40:60**	**CTN 40:60**
1	Carbon (***C***)	57.92	29.30	32.21
2	Oxygen (***O***)	23.81	24.85	27.10
3	Nitrogen (***N***)	11.77	14.71	16.57
4	Calcium (***Ca***)	1.14	23.32	16.38
5	Sodium (***Na***)	0.00	0.58	1.89

	Total	**94.64**	**92.76**	**94.15**

From the EDX analyses, raw crab shell (CRS) showed a high Calcium (Ca) content of 23.32 wt%. Following chemical treatment to produce chitin (CTN), the Ca content dropped to 16.38 wt%. The SEM image in Fig 3.1 below shows a relatively smooth and homogeneous surface, characteristic of a neat unreinforced thermosetting polymer. The relatively uniform grey tone indicates a homogeneous material phase without the complex inclusion of secondary fillers. The absence of distinct phase separation or filler particles confirmed the baseline morphology of the pristine UPE matrix. SEM images in Fig 3.2 for CRS composite revealed a fragmented and rocky interface. There were visible gaps (voids) between the raw shell particles and the UPE matrix, explaining the poor mechanical strength. The CTN interface in Fig 3.3 below appeared more integrated. While some fragmentation remained, the chemical cleaning of the chitin surface allowed for a more stitched appearance, where the resin successfully encapsulated the chitin particles. This indicates a demineralization efficiency that successfully reduced the rocky inorganic mineral phase as shown in the SEM images Fig 3.1- Fig 3.3 below.

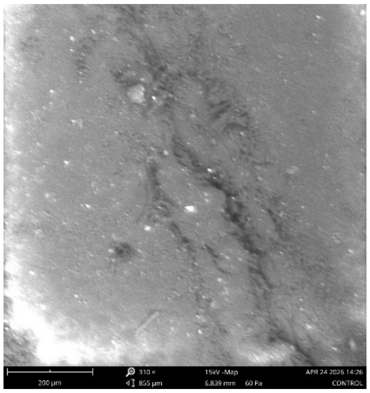

Fig 3.1: Control UPE

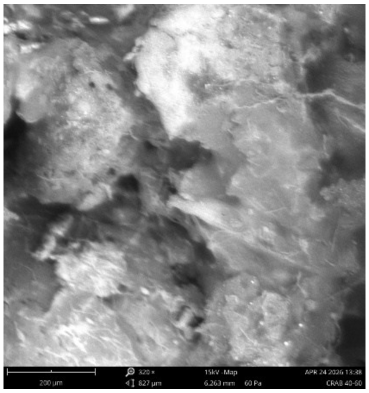

Fig 3.2: CRS composite

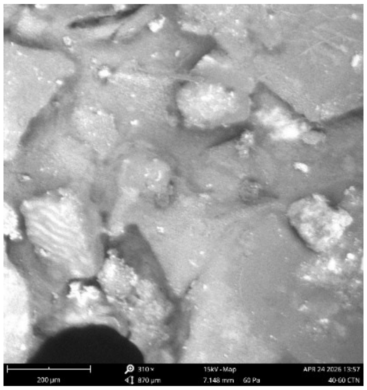

Fig 3.3: CTN composite

4.1 FTIR Analysis

The spectrum for CRS showed strong carbonate CO_3^{-2} bands. In the CTN spectrum, these bands were significantly attenuated, replaced by sharper amide I and amide II bands, confirming the emergence of a purified chitin structure. The FTIR spectra for the CRS and CTN is shown below;

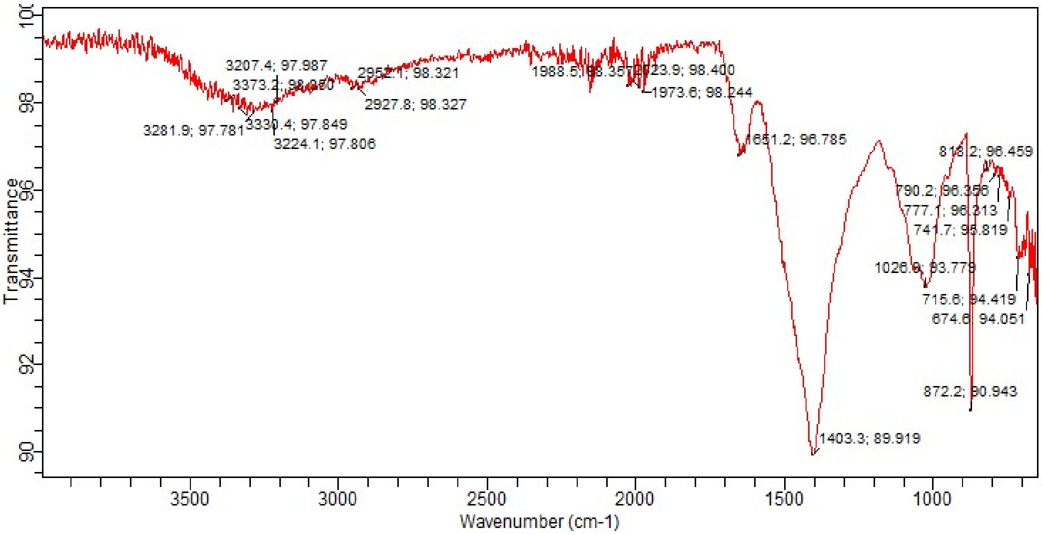

Fig 4.1: FTIR spectra of Crab shell

The results of the FTIR for the crab shell was summarized in Table 4.1 below. The raw crab shell spectrum (Fig 4.1) displays a complex profile due to its composite nature: a matrix of chitin fibres embedded in a protein (mainly calcium-binding proteins) and calcium carbonate ($CaCO_3$) in the form of calcite or aragonite.

Table 4.1: Summary of FTIR band assignments for extracted Crab shell (CRS)

Wavenumber (cm^{-1})	Functional group	Assignment
3430	O–H, N–H stretching	Overlapped hydroxyl (from chitin) and amide A (from protein)
2952.1	C–H stretching (asymmetric)	CH_2 in chitin and protein side chains
2927.8	C–H stretching (symmetric)	CH_2
1988.2	C=O (carbonate)	Calcium carbonate – diagnostic of shell mineral
1973.6	C=O stretching (amide I)	Protein secondary structure (α-helix/β-sheet)
1651.2	N–H bending (amide II)	Protein and chitin N-acetyl groups

Wavenumber (cm⁻¹)	Functional group	Assignment
1403.3	CH_2 bending	CH_2OH group of chitin
1380	CH_3 symmetrical deformation	Amide III (N-acetyl group)
1083–1034	C–O stretching	Pyranose ring vibrations
701	Ring breathing	β-1,4-glycosidic linkage (characteristic of chitin)

From the Table 4.1 above. The instrument parameter 1798 cm^{-1} for Carbonate (CO_3^{2-}) from Carbonate band $CaCO_3$ in the data file corresponds to the carbonate reference in the raw crab shell. In raw crab shell spectra, a strong band typically appears around 1988.5 –1973.6 cm^{-1} (C=O stretching of carbonate). This band is absent in the chitin spectra (as shown in Fig. 4.2 below).

Furthermore, at 1651.2 cm^{-1} C=O stretching of Amide I. This band is dominated by the C=O stretching vibration of the peptide bonds in proteins. It also receives a contribution from the C=O of the N-acetyl groups of chitin. In raw shell, the high intensity (low transmittance) indicates abundant protein content.

Fig.: 4.2 FTIR of Chitin (CTN)

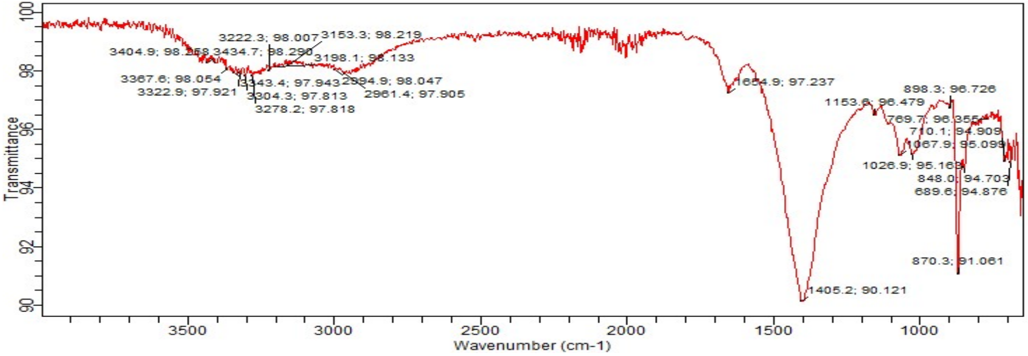

After sequential demineralization and deproteinization, the resulting chitin spectrum (Fig. 4.2) shows significant changes: the complete disappearance of the carbonate band and a marked reduction in amide II intensity, confirming removal of $CaCO_3$ and proteins. The result of the Chitin analysis is shown in Table 4.3 below;

Table 4.2: Summary of FTIR band assignments for extracted chitin

Wavenumber (cm⁻¹)	Functional group	Assignment
3404.0	O–H, N–H stretching	Hydrogen-bonded (crystalline chitin)
3322.9	N–H stretching (amide A)	Secondary amide, intermolecular H-bonding
3224.1	C–H stretching (aromatic)	Possibly residual pigment or cross-links
2994.9 –2961.4	C–H stretching	CH_2
1654.9	C=O stretching (amide I)	N-acetyl group of chitin
1405.2	CH_2 bending	CH_2OH
1153.8	CH_3 deformation	Amide III (N-acetyl)
1026.9 – 870.3	C–O stretching	Mono-substituted aromatic ring

The most striking difference from the raw shell spectrum is the complete absence of the $CaCO_3$ band. This confirms that the demineralization step was highly effective, Jabeen et al. (2023) reported identical results for chitin extracted from *Callinectes sapidus* shells, with no residual carbonate peaks confirming that demineralization successfully removed calcium carbonate. Zhou et al. (2024) similarly reported the disappearance of the 1798 cm^{-1} band after acid treatment of crab shells.

At Amide I (1654.9 cm^{-1}) and Amide II (1580 cm^{-1}) indicated the presence of chitin, both bands are retained but the amide II band is less strong compared to raw crab shell, because proteins contributed significantly to amide II in the raw sample.

4.3 Mechanical Performance

A clear distinction was observed between the raw shell and chitin reinforcements as shown in the Table 4.3 below:

Table 4.3 Mechanical Properties of the CRS and CTN reinforced UPE Composites

S/N	Filler	Filler: Matrix ratio (%)	Vickers Hardness (HV)	Tensile Strength (Mpa)	Elongation @ break (%)	Flexural Strength (Mpa)
1	control	0	19.10	48.72	8.71	0.07
2	Crab Shell (CRS)	40:60	47.20	92.39	8.33	2.86
3	Chitin (CTN)	40:60	53.36	176.50	2.32	2.20

The transition from raw Crab Shell (CRS) to Chitin (CTN) nearly doubles the tensile strength (from 92.39 MPa to 176.50 MPa). This indicates that removing the protein and mineral layers from the shell allows for much better stress transfer between the filler and the matrix.

The hardness result showed that Chitin composite is the harder than CRS by few points 53.36 HV, but it shows a sharp drop in Elongation at Break (2.32%). This suggests that while chitin makes the material much stronger and stiffer, it also makes it more brittle compared to the raw shell. The Flexural Strength is slightly lower for Chitin (2.20 MPa) than for the Raw Shell (2.86 MPa). This could imply that the raw shell's mineral content (calcium carbonate) provides better resistance to bending forces, even if it is weaker under pure tension. Interestingly, both fillers massively outperform the Control (Neat Resin) in all properties tested, especially in tensile and flexural strength, proving that crab waste is a highly effective reinforcement.

4.4 Thermal Stability (TGA/DTA)

The thermal results is shown in Table 4.4 below, it describes the effect of temperature on the mass of the prepared composites:

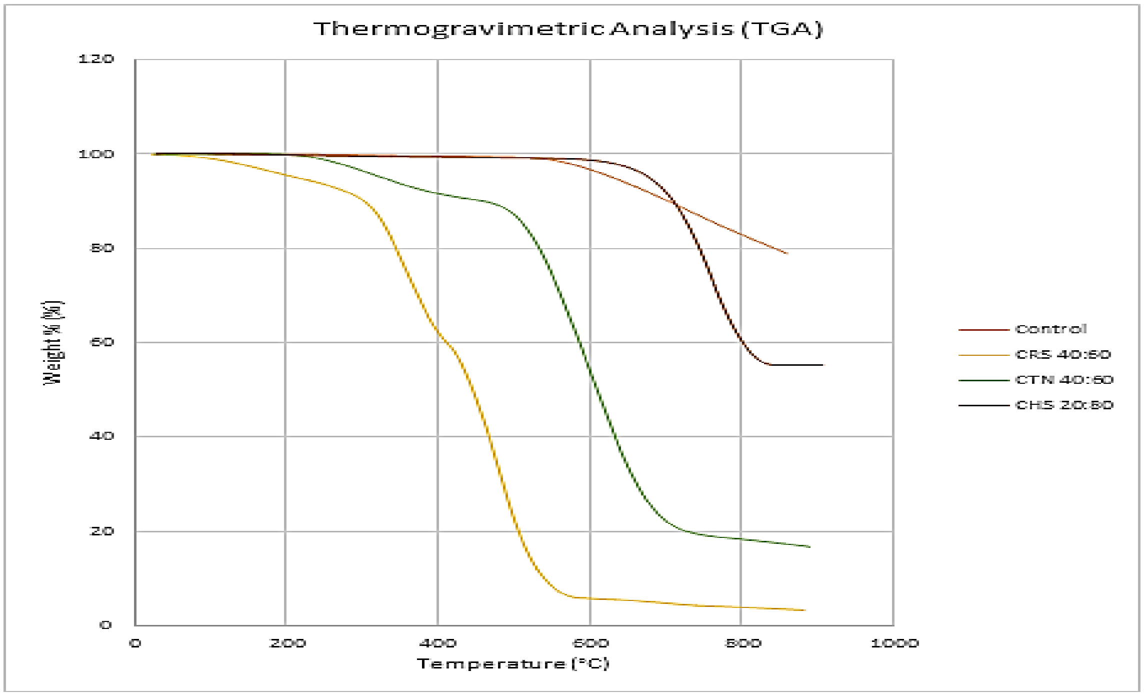

Fig 4.3: TGA thermogram for the prepared composites

From the graph above, the result is summarized in Table 4.4 below;

Table 4.4: Thermogravimetric Analysis Data Summary

S/N	Sample	T_{onset} (°C)	T_{max1} (°C)	T_{max2} (°C)	Residual Weight at >800°C (%)
1	Control (Pure UPE)	≈ 560	NA	NA	≈ 80 (at 850°C)
2	CRS 40:60 (Crab Shell)	≈ 150	≈ 380	≈ 520	≈ 4
3	CTN 40:60 (Chitin)	≈ 260	≈ 320	≈ 580	≈ 18

In the TGA analysis, the CRS 40:60 sample showed early weight loss (T_{onset} (°C) ≈ 150°C), and in the DTA, it showed a peak1 at ≈ 210°C. The chemical removal of proteins and calcium carbonate to produce Chitin (CTN) eliminated the low-temperature triggers. By removing these impurities, it successfully pushed the onset temperature from ≈ 150°C (CRS 40:60) to ≈ 250°C (CTN 40:60). The Onset Temperature marks the threshold where the material's chemical bonds begin to break significantly. In this study, the early T_{onset} (°C) for the 40% reinforced samples (CRS 40:60 starting at ≈ 150°C and CTN 40:60 at ≈ 250°C) indicates that the bio-filler is the weak link. The Crab shell and Chitin bio-fillers at 40% loading significantly lower the thermal stability of the composite compared to the Control. This is likely due to the high organic/mineral content of the fillers acting as a thermal bridge, accelerating the degradation of the polymer matrix. Further understanding of the thermal curve is shown in the DTA analysis in the figure 4.7 below and summarized in the Table 4.5 below.

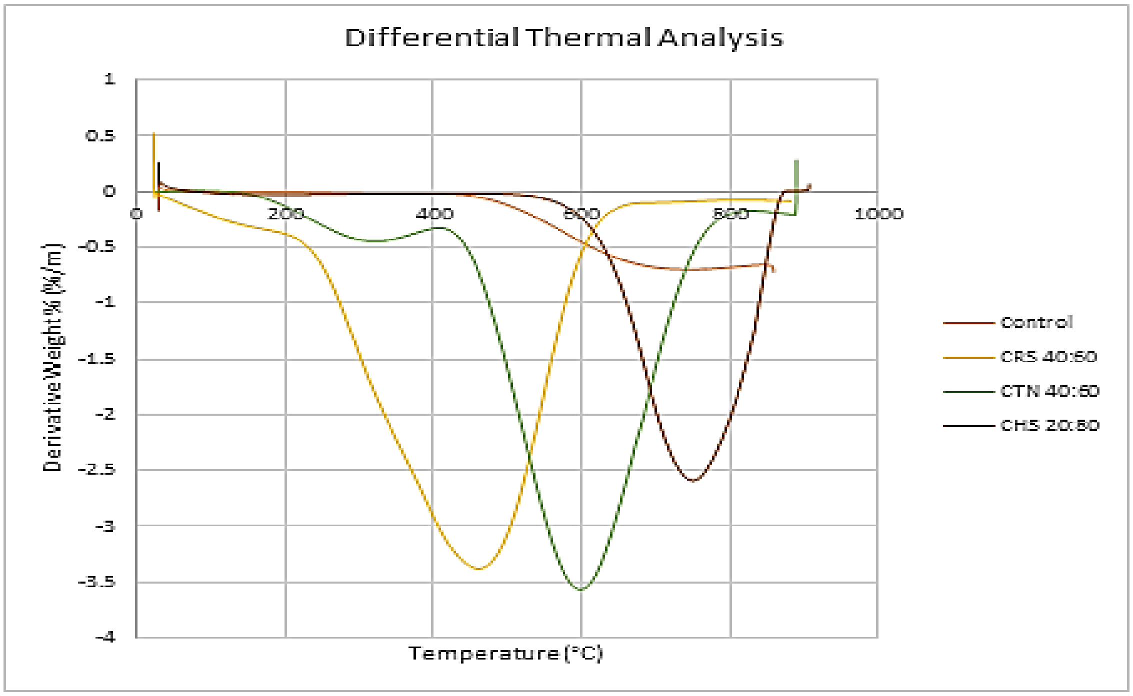

Fig 4.4: DTA thermogram for the prepared composites

Table 4.5 DTA analysis table

S/N	**Sample**	***Peak1* (%/m)**	***Peak2* (%/m)**	***Peak3*(%/m)**	**Rate of Loss (Intensity)**
1	Control (Pure UPE)	N/A	N/A	≈ 810°C	Low & Broad
2	CRS 40:60 (Crab Shell)	≈ 210°C	≈ 450°C	≈ 680°C	Very High (Steep)
3	CTN 40:60 (Chitin)	≈ 340°C	≈ 600°C	≈ 780°C	Highest (Sharp)

The DTA shows that the first major breakdown for CTN 40:60 is delayed to 340°C, proving that purified chitin is inherently more stable than the raw crab shell. At 40% loading, there is a lack of sufficient UPE resin to fully wet and encapsulate every filler particle. This creates a high density of filler-filler contacts and interfacial voids. When the degradation temperature is reached, these voids act as thermal channels, allowing heat and oxygen to penetrate the composite almost instantly. This leads to the rapid collapse seen as a deep DTA peak. In the CRS 40:60 sample specifically, the 40% loading includes a large amount of calcium carbonate and residual proteins. As these decompose, they act as a catalyst or triggering a chain reaction that accelerates the breakdown of the surrounding UPE. The deep peak at ≈450°C for CRS 40:60 is a visual representation of this accelerated degradation.

In the CTN 40:60 sample, Peak 1 (≈ 340°C) represents the degradation of the chitin chains, Peak 2 (≈ 600°C) is the main decomposition of the UPE. While it is more stable than CRS, the peak is very sharp and deep, meaning once the material starts to fail, it fails rapidly. The CTN peak is the deepest (reaching -3.5 %/m), indicating a violent and fast degradation. The raw shell acted as a thermal pro-degradant. The high mineral content caused the UPE matrix to break down at lower temperatures, likely due to the catalytic effect of the minerals on the polyester chains. Purified chitin showed a more stable degradation. By removing the volatile proteins and unstable minerals, the chitin-reinforced composite retained more mass at higher temperatures (18%) compared to the raw shell composite (4%).

Table 4.6: Comparative Data for CRS and CTN

Sample Type	**Hardness (HV)**	**Tensile Strength (MPa)**	**Thermal Stability**	**Morphology**
Neat UPE (Control)	19.10	48.72	Baseline	Homogeneous
CRS 40:60 (Crab Shell)	47.20	92.39	Pro-degradant (Lower)	Fragmented/Rocky
CTN 40:60 (Chitin)	53.36	176.50	More Stable than raw Crab shell	Integrated

Conclusion

The study confirms that while raw crab shell can be used as a low-cost filler, its high mineral and protein content limit its performance. The Table 4.6 above gives a summary of the comparative properties of the two fillers, CRS and CTN. We therefore conclude that, chemical refinement of the raw Crab shell into chitin is essential to improve mechanical properties such as hardness and tensile strength, thermal stability and increase in interfacial bonding, making it a superior choice for semi-structural applications.

References

Abdou, E. S., Nagy, K. S. A., & Elsabee, M. Z. (2008). Extraction and characterization of chitin and chitosan from local sources. Bioresource Technology, 99(5), 1359–1367.

Akarue, O., & Akarue, B. O. (2020). Utilization of crab shells as fertilizer on the growth of Amaranthus hybridus. Journal of Applied Sciences and Environmental Management, 24(6), 1031–1035.

Demir, H., Atikler, U., Balköse, D., & Tıhmınlıoğlu, F. (2006). The effect of fiber surface treatments on the tensile and water sorption properties of polypropylene–luffa fiber composites. Composites Part A: Applied Science and Manufacturing, 37(3), 447–456.

Faruk, O., Bledzki, A. K., Fink, H.-P., & Sain, M. (2012). Biocomposites reinforced with natural fibers: 2000–2010. Progress in Polymer Science, 37(11), 1552–1596.

Islam, M. M., Khan, A. M., & Islam, M. M. (2011). Chemical characterization of chitin and chitosan extracted from shrimp shells. Journal of Polymers and the Environment, 19(1), 97–103.

Ku, H., Wang, H., Pattarachaiyakoop, N., & Trada, M. (2011). A review on the tensile properties of natural fiber reinforced polymer composites. Composites Part B: Engineering, 42(4), 856–873.

Kucukgulmez, A., Celik, M., Yanar, Y., Ersoy, B., & Candan, C. (2011). Physicochemical characterization of chitin extracted from Metapenaeus stebbingi shells. Food Chemistry, 126(3), 1144–1148.

Kumirska, J., Czerwicka, M., Kaczyński, Z., Bychowska, A., Brzozowski, K., Thöming, J., & Stepnowski, P. (2020). Application of spectroscopic methods for structural analysis of chitin and chitosan. *Marine Drugs*, 8(5), 1567–1636.

Musmade, N. A., & Mahatma, L. (2021). Extraction and Characterization of Chitosan by Simple Technique from Mud Crabs (Scylla serrata Forskal). International Journal of Current Microbiology and Applied Sciences, 10(6), 464-474.

Mohanty, A. K., Vivekanandhan, S., Pin, J.-M., & Misra, M. (2018). Composites from renewable and sustainable resources: Challenges and innovations. Science, 362(6414), 536–542.

Muzzarelli, R. A. A. (1977). Chitin. Pergamon Press.

Nwosu, M. C., Ugwuegbu, D. C., & Ekele, I. (2022). Characterization of unsaturated polyester composites filled with chemically modified crab shell particles. Nigerian Journal of Technology, 41(2), 215–223.

Oladele, I. O., Agbabiaka, O. G., Adediran, A. A., Akinwekomi, A. D., & Balogun, A. O. (2019). Structural performance of poultry feather fibre and snail shell reinforced epoxy matrix hybrid composites.

Onuegbu, T. U., Umoh, E. T., & Ugele, I. N. (2011). Mechanical properties of snail shell ash filler reinforced unsaturated polyester composites. Academic Research International, 1(3), 255–260.

Pillai, C. K. S., Paul, W., & Sharma, C. P. (2009). Chitin and chitosan polymers: Chemistry, solubility and fiber formation. Progress in Polymer Science, 34(7), 641–678.

Ramesh, M., Palanikumar, K., & Reddy, K. H. (2017). Plant fibre based bio-composites: Sustainable and renewable green materials. Renewable and Sustainable Energy Reviews, 79, 558–584. https://doi.org/10.1016/j.rser.2017.05.094

Rinaudo, M. (2006). Chitin and chitosan: Properties and applications. Progress in Polymer Science, 31(7), 603–632.

Sanjay, M. R., Arpitha, G. R., Yogesha, B., Senthamaraikannan, P., Senthil, S., & Pradeep, S. (2018). An overview of natural fiber reinforcements for polymer matrix composites. Science and Technology of Advanced Materials, 19(1), 256–270.

Yan, N., & Chen, X. (2015). Sustainability: Don't waste seafood waste. Nature, 524(7564), 155–157

. Journal of Public Policy and Administration, 16(4), 201–215.